This is the accepted manuscript made available via CHORUS. The article has been published as:

Isotopic Disorder: The Prevailing Mechanism in Limiting the Phonon Lifetime in Hexagonal BN

Ramon Cuscó, James H. Edgar, Song Liu, Jiahan Li, and Luis Artús

Phys. Rev. Lett. **124**, 167402 — Published 22 April 2020

DOI: 10.1103/PhysRevLett.124.167402

Isotopic disorder: the prevailing mechanism in limiting the phonon lifetime in hexagonal BN

Ramon Cuscó

Institut Jaume Almera (ICTJA-CSIC), Consejo Superior de Investigaciones Científicas, Lluís Solé i Sabarís s.n., 08028 Barcelona, Spain

James H. Edgar, Song Liu, and Jiahan Li

Tim Taylor Department of Chemical Engineering, Kansas State University, Manhattan, Kansas 66506, USA

Luis Artús

Institut Jaume Almera (ICTJA-CSIC), Consejo Superior de Investigaciones Científicas, Lluís Solé i Sabarís s.n., 08028 Barcelona, Spain

Abstract

The phonon line width of isotopically controlled h-BN single crystals has been determined by Raman scattering. The scattering by isotopic mass disorder induces a phonon broadening that is largest for boron 11 fractions around 0.65. Lowest-order perturbation theory does not suffice to explain the dependence of the isotopic broadening on isotopic composition. A multiple-scattering theory based on the coherent potential approximation provides a good quantitative account of the phonon shift and broadening with isotopic composition observed in the experiments. Isotopic disorder scattering is shown to have a prominent role in limiting the optical-phonon lifetime in h-BN

PACS numbers: 78.30.-j,63.20.Ry,63.22.Np

Isotope-engineering of layered two-dimensional (2D) crystals aimed at tuning the physical properties of the material is currently attracting a great deal of interest [1–4]. The degree of freedom associated with the nuclear mass and the effects of isotopic disorder in the crystal provide new opportunities to tailor the novel physics emerging from van der Waals layered materials [5]. Isotope control mainly influences the phonons of the lattice, which are collective excitations whose energies and lifetimes govern the thermal conductivity κ. Modification of 2D thermal conductivity by isotope-engineering was first realized in graphene [1], and recently, a large boost in thermal conductivity has been reported in 2D MoS_2 monolayers [3]. Changes in the optical emission properties of isotopically enriched crystals may also be induced via electron-phonon interaction [2, 4, 6].

Hexagonal boron nitride (h-BN) has a prominent role in the family of 2D van der Waals materials because its similarity with graphene makes it an optimal substrate for graphene and permits a seamless integration in atomically thin heterostructures [5, 7]. Additionally, the highly anisotropic h-BN crystal displays exceptional dielectric properties[8] that can be exploited in nanophotonics for confining electromagnetic radiation to length scales below the diffraction limit [7, 9]. h-BN is a low-loss natural hyperbolic material which, owing to its two well-separated reststrahlen bands associated with in-plane and out-of-plane modes [10], supports type I and type II phonon polaritons [11]. Isotopically enriched BN crystals are particularly interesting for polaritonic applications, since a threefold increase in phonon-polariton propagation length and the presence of higher-order modes were demonstrated in isotopically enriched ^{10}BN samples owing to reduced isotopic-disorder scattering [12].

h-BN exhibits two Raman active modes, which have E_{2g} symmetry. The low-energy mode E_{2g}^{low} is a shear mode involving the gliding motion of the weakly bound honeycomb layers. This particular mode exhibits an extremely narrow linewidth [13] well below the spectrometer bandwidth, which makes it unsuitable for a Raman scattering study of isotopic effects on the phonon linewidth. The high-energy mode E_{2g}^{high} involves *in-plane* vibrations of boron against nitrogen and lays in a spectral region with high density of phonon states. Anharmonic decay and E_{2g}^{high} phonon lifetimes were investigated in detail in natural and isotopically pure h-BN by means of temperature-dependent Raman scattering measurements, which showed a significant increase of the E_{2g}^{high} phonon lifetime in isotopically pure ^{10}BN and ^{11}BN samples [14]. In that work, lowest-order perturbation theory was used to describe the isotopic-disorder-induced broadening of the Raman line width in the natural h-BN sample. The strength of isotopic-disorder-

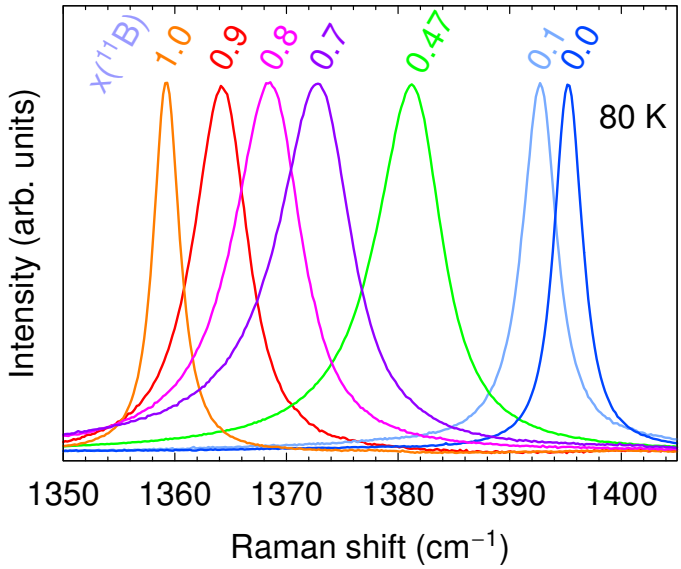

FIG. 1. (a) High-resolution Raman spectra of the E_{2g}^{high} mode for h-BN samples at several ^{11}B concentrations x ranging from 0 to 1 at 80 K.

induced phonon self-energy is characterized by the mass variance [15]

$$g_2(x) \approx \left(\frac{\delta m}{m}\right)^2 x(1-x), \tag{1}$$

where $m = 10.012937$ u is the mass of the lighter isotope, $\delta m = 0.996368$ u is the mass difference between the two stable boron isotopes, and x is the fraction of the heavier isotope. Given the large mass variance taking place in isotopically disordered BN, lowest-order perturbation theory may not suffice to fully account for the Raman line width in isotopically disordered samples. A generalization to higher orders of perturbation theory was given in Ref. [15]. This formalism suggested that the third-order contribution, which is antisymmetric with respect $x = 0.5$, could account for the asymmetry in the phonon line-width dependence on x, as experimentally observed in isotopically disordered C [16, 17] and SiC [18]. An alternative description of isotopic disorder based on the coherent potential approximation (CPA) [19], which includes multiple scattering in a self-consistent way, has proven successful in quantitatively accounting for the Raman line-width dependence on isotopical composition in isotopically disordered ^{12}C/^{13}C samples [16, 17].

To elucidate the role of isotopic disorder in limiting the optical-phonon lifetime in h-BN, in this letter we investigate the Raman-active E_{2g}^{high} phonon on a set of isotopically controlled h-BN samples spanning the whole composition range, with ^{11}B fractions $x = 0$, 0.1, 0.47, 0.7, 0.8,

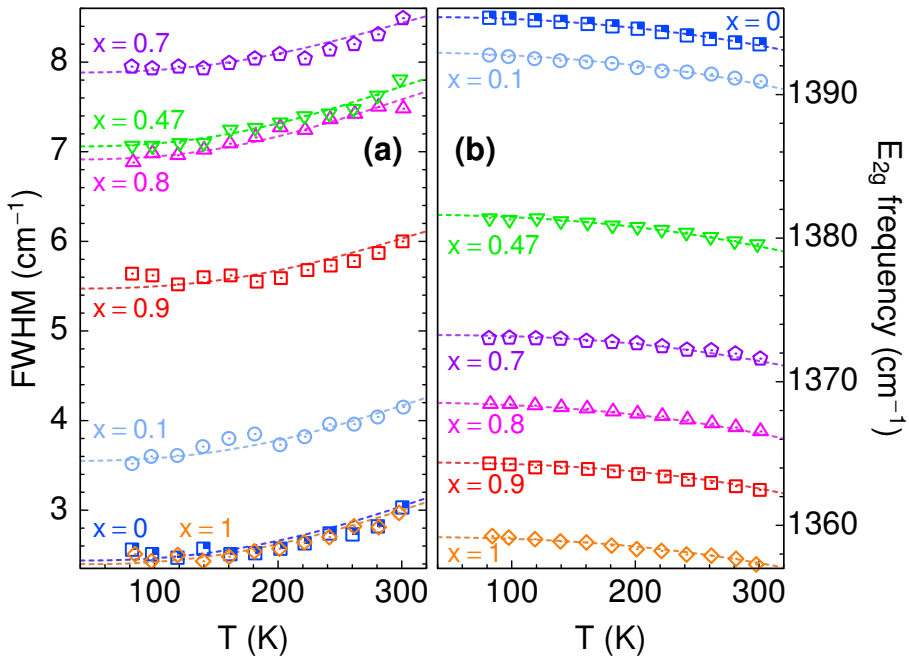

FIG. 2. Temperature dependence of the line width (a) and frequency (b) of the E_{2g}^{high} phonon from room temperature to 80 K. Symbols are Raman scattering measurements and lines are fits to the anharmonic decay model described in Refs. [14, 22]

0.9, and 1. This study was performed on isotopically enriched h-BN crystals grown from high-purity elemental ^{10}B (99.2 at%) or ^{11}B (99.4 at%) powder by using metal flux method. Growth details are given elsewhere [14, 20]. The Raman scattering measurements were carried out in backscattering configuration from the c face using the 514.5-nm line of an Ar^+ laser. The scattered light was analyzed using a Jobin-Yvon T64000 triple spectrometer equipped with a LN_2-cooled charge-coupled device (CCD) detector, with a spectral bandwidth of ~ 0.7 cm^{-1}. First-principle phonon calculations were performed in the framework of density functional perturbation theory in the local density approximation (LDA) as implemented in the ABINIT package [21]. Calculation details and the underlying theory used to evaluate the thermal expansion, anharmonicity, and isotopic disorder effects are given in Ref. [14, 22].

Raman spectra at 80 K of the E_{2g}^{high} mode of h-BN samples for a number of ^{11}B concentrations spanning the whole concentration range are shown in Fig. 1. The isotopically pure samples display narrow line widths (~ 2.4 cm^{-1}) which are essentially limited by the anharmonic decay of the phonons and scattering with impurities. When isotope mixing is introduced, the Raman lines visibly broaden and the frequencies gradually evolve from the values in the pure crystals.

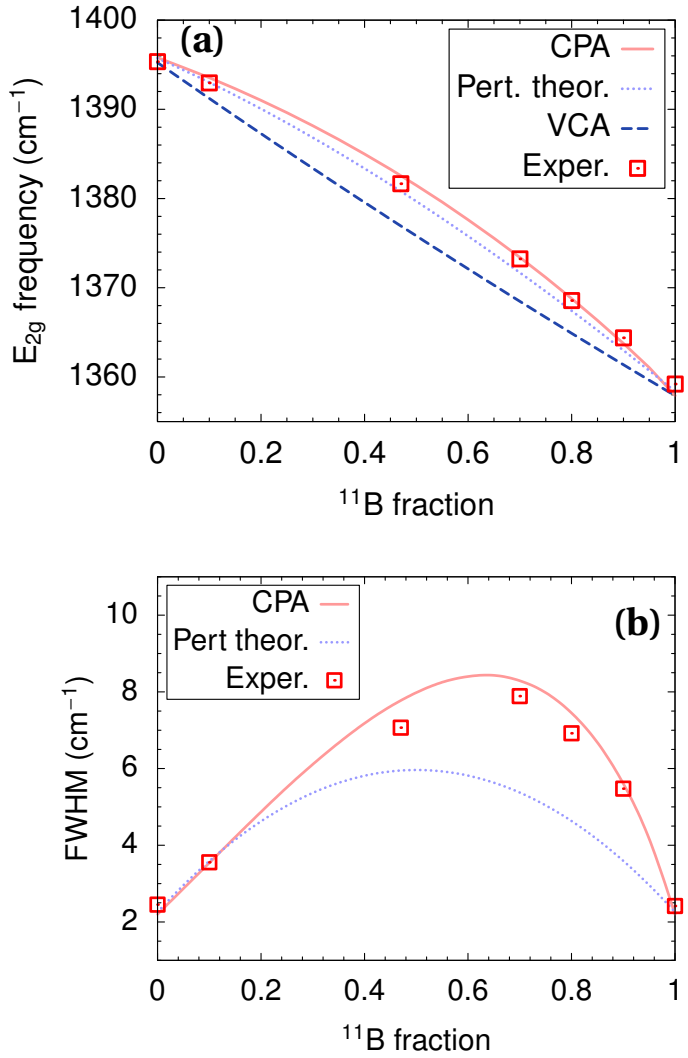

FIG. 3. Dependence on isotopic composition of (a) the frequency and (b) the FWHM of the E_{2g}^{high} phonon in isotopically controled h-BN. Symbols are experimental values from Raman scattering measurements. The solid and dotted lines are, respectively, the results of the CPA and third-order perturbation theory calculations. The composition dependence of the phonon frequency predicted by the virtual crystal approximation is indicated by a dashed line.

It is worth noticing that a small amount admixture of the lighter ^{10}B isotope in a ^{11}BN host lattice ($x = 0.9$ sample) produces a much larger effect on the phonon line shape than the opposite situation ($x = 0.1$). Furthermore, the sample with roughly equal concentrations of lighter and heavier isotopes ($x = 0.47$), in which one could naively expect the highest degree of disorder, displays a narrower line width than that of the $x = 0.7$ sample. This observation contradicts Eq. (1), which is a symmetric function with a maximum at $x = 0.5$.

A theory of anharmonic processes in crystals with isotopic impurities was developed by Maradudin and Califano [23]. It was found that the contributions to the shift and broadening of the phonon from the isotopic impurities alone is temperature independent, while the terms involving anharmonicity are temperature dependent [23]. Then, the contribution of isotopic-disorder-induced scattering to the Raman line width can be separated from the phonon anharmonic decay contribution by analyzing the temperature dependence of the E_{2g}^{high} Raman peak. Figure 2 shows the E_{2g}^{high} phonon line width (a) and frequency (b) as a function of temperature for all the samples studied. The FWHM and frequency values plotted in Fig. 2 were obtained by fitting asymmetric Lorentzian line shapes to the Raman spectra of Fig.1, taking into account the convolution with the spectral response of the spectrometer, which was determined by measuring the 692.947 nm line of a Hg calibration lamp. The spectral response correction to the FWHM is less than 4%. As one could expect from the VCA, the frequencies in Fig. 2(b) display a gradual decrease as the ^{11}B fraction increases from $x = 0$ to $x = 1$. Interestingly, Fig. 2(a) clearly shows that the FWHM is highest for the $x = 0.7$ sample, whereas the width of the sample with roughly the same concentration of ^{10}B and ^{11}B ($x = 0.47$) is quite similar to that of the $x = 0.8$ sample, where the mass variance is substantially lower. The experimental values were fitted to the anharmonic decay model described in Ref. [14, 22]. The anharmonic decay effective potentials we find for the isotopically controlled samples are consistent with those reported in Ref. [14], with basically the same cubic anharmonic coefficients and a quartic anharmonic coefficient gradually increasing from ^{10}BN to ^{11}BN. The same background impurity broadening ($\Gamma_i \approx 1.3$ cm^{-1}), corresponding to that found for the isotopically pure samples [14], was used for all isotopic compositions in the calculations. The model fit allows us to extrapolate the full width at half maximum (FWHM) and frequency values to low temperature and to average out experimental errors in their determination from the Raman spectra. In the isotopically pure samples, the FWHM at low temperature is ~ 2.4 cm^{-1}. Then, by subtracting this value to the FWHM measured from the Raman spectra, we extract the purely isotopic contribution to the line width.

Since the lowest-order perturbation theory [see Eq. (1)] does not account for the observations, first we consider the third-order corrections to the imaginary part of the isotopic-disorder-induced phonon self-energy [15]

$$\Gamma_3(\omega) = 4\frac{g_3(x)}{g_2(x)}\frac{\Delta_2(\omega)}{\omega g_2(x)}\Gamma_2(\omega), \tag{2}$$

where $g_3(x) \approx (\delta m/m)^3 x(1-x)(2x-1)$, and $\Delta_2(\omega)$ and $-\Gamma_2(\omega)$ are, respectively, the real and imaginary parts of the phonon self-energy to second order. The latter were evaluated in Ref. [14], so it is straightforward to include the third-order corrections to the phonon line width by using Eq. (2). Note that $g_3(x)/g_2(x) \approx (\delta m/m)(2x-1)$, whose absolute value is in the order of 5×10^{-2} at the extrema ($x = 0.25$ and $x = 0.75$). On the other hand, $\omega g_2(x)$ is in the order of 2 for the E_{2g}^{high} frequency, and $\Delta_2(\omega)$ is typically below 2 cm^{-1}, so the third-order correction given by Eq. (2) is very small, in the order of $\Gamma_3/\Gamma_2 \lesssim 10^{-1}$. Thus, while the functional dependence on x of the phonon self-energy up to third-order in perturbation theory may fit the observations as suggested in Ref. [15], the magnitude of the third-order terms is too small to quantitatively account for the asymmetric dependence of the FWHM vs. isotopic composition measured in h-BN.

Given the large relative mass fluctuation in BN and the high phonon density of states (PDOS) around the E_{2g}^{high} mode, large self-energy corrections due to isotopic disorder are expected for the E_{2g}^{high} mode. Then, an approach based on CPA [19], which is a multiple scattering formalism that treats the isotopically disordered crystal as a self-consistent effective medium, may provide a more accurate description of isotopic disorder effects. The medium is characterized by a dimensionless self-energy $\tilde{\varepsilon}(\omega)$, which describes the phonon correction due to a mass-defect single site relative to a virtual crystal (VC) with an isotopic-composition averaged cation mass $M = (1-x)m + x(m+\delta m)$. The CPA, which was originally developed for mixed binary alloys [19], was later generalized to mixed diatomic crystals by treating $\tilde{\varepsilon}(\omega)$ and the site Green's function $G(\omega^2)$ as matrices [24]. It was shown that for a mixed diatomic chain with disorder restricted to sublattice 1, only the (1,1) element of $\tilde{\varepsilon}(\omega)$ is nonzero [24]. Assuming a diagonal self-energy $\tilde{\varepsilon}_{\alpha\beta} = \delta_{\alpha 1}\delta_{\beta 1}\tilde{\varepsilon}$ for the lamellar structure of h-BN, where all the atomic motions of the phonon eigenvectors are aligned along one of three orthogonal directions, the Green's function for the single site in the effective medium can be evaluated as

$$G(\omega^2) = \frac{1}{M}\int_0^\infty \frac{g_{\text{VC}}(\xi)}{\omega^2[1-\tilde{\varepsilon}(\omega)] - \xi^2} d\xi, \tag{3}$$

where $g_{\text{VC}}(\omega)$ is the PDOS for the VC projected to the disordered cation sublattice and normalized to unity. The PDOS was calculated for the isotopically pure ^{11}BN crystal using the ABINIT package and it was extrapolated to arbitrary isotopic compositions by frequency scaling according to the square root of the reduced mass. The CPA self-consistency condition requires

that the average scattering from the single site vanishes, which can be expressed as [16]

$$M\tilde{\varepsilon}(\omega) = \frac{x(1-x)(\delta m)^2\omega^2 G(\omega^2)}{1+\omega^2[(1-2x)\delta m + M\tilde{\varepsilon}(\omega)]G(\omega^2)}. \tag{4}$$

Equations (3) and (4) are iteratively solved until a self-consistent $\tilde{\varepsilon}(\omega)$ is found. This determines the phonon frequency shift $\tilde{\omega} = \omega[1-\mathrm{Re}\,\tilde{\varepsilon}(\omega)]^{-1/2}$ and the FWHM broadening $-\tilde{\omega}\,\mathrm{Im}\,\tilde{\varepsilon}(\tilde{\omega})$ due to isotopic disorder.

In Fig. 3, we compare the experimental values of E_{2g}^{high} frequency and isotopic-disorder-induced broadening with the results of the CPA and third-order perturbation theory calculations. The calculated frequencies have been vertically downshifted to match the experimental points so as to compensate for the slight overestimation of phonon frequencies by the *ab-initio* LDA calculations [22], which nevertheless accurately predict the difference between the phonon frequencies of isotopically pure ^{10}BN and ^{11}BN in the virtual crystal approximation (VCA). For the isotopically mixed crystals, the phonon frequency exhibits a positive bowing, with an isotopic-disorder-induced shift of ~ 3.9 cm^{-1} for natural composition ($x = 0.8$) and of ~ 5.6 cm^{-1} for $x = 0.47$ relative to the VCA values. Both CPA and perturbation theory calculations predict this bowing, but the latter tend to underestimate the phonon shift. The phonon frequency dependence reported in Fig. 3 provides an accurate calibration for the determination of isotopic composition in h-BN from Raman scattering measurements.

In Fig. 3 (b) we plot the FWHM values determined from asymmetric Lorentzian fits to the Raman spectra. As already seen in the temperature dependence analysis [Fig. 2 (a)], the isotopic broadening is highest for the $x = 0.7$ sample, with Δ(FWHM) ~ 5.5 cm^{-1}, and increases much more steeply when ^{10}BN impurities are introduced in a ^{11}BN host than conversely. The asymmetric dependence of the FWHM on x is well predicted by the CPA calculations, which also provide a good quantitative account of the observed broadening. In contrast, calculations up to third-order perturbation theory yield a symmetric dependence on x and clearly underestimate the isotopic disorder broadening. A much higher third-order contribution would be required to simulate the asymmetric x dependence observed in the experiments. Such a large third-order contribution would itself question the validity of the perturbation theory approach. Interestingly, studies of phonon transport in ultrathin graphite have highlighted the important role of wave interference effects as a result of multiple scattering events in 2D high-κ materials where isotope scattering is important [25]. κ values differing by a factor of 2 in relation to the incoherent, independent scattering model have been predicted in C and BN nanotubes [26]. The

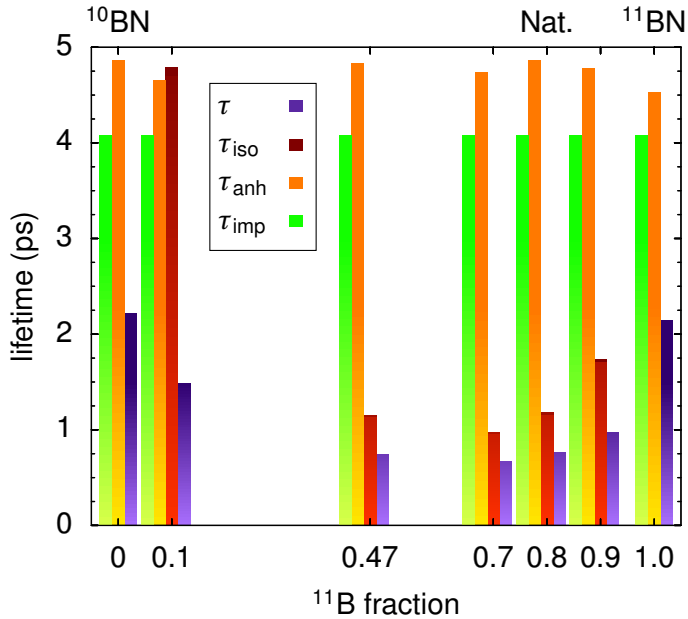

FIG. 4. E_{2g}^{high} phonon lifetimes (τ) measured at 80 K and the corresponding lifetimes associated with the different decay pathways: anharmonic (τ_{anh}), isotopic disorder (τ_{iso}), and impurity scattering (τ_{imp}), for the isotopically controled h-BN samples.

present study shows that consideration of multiple scattering is also necessary to account for the isotopic disorder scattering rates in the E_{2g}^{high} phonon of BN. Given the large isotopic mass ratio for boron, isotopic effects are expected to be important in BN, and the multiple scattering effects should probably be even more marked in h-BN than in ultrathin graphite.

We note that, for the natural composition ($x \sim 0.8$) usually considered in studies of h-BN, the measured isotopic broadening is ~ 2.3 cm^{-1} higher than the perturbation theory result. This explains that a higher value of the background impurity damping had to be included to account for the experimental FWHM values in Ref. [14], since the isotopic disorder contribution was estimated using lowest-order perturbation theory. In fact, the difference between the background impurity damping parameters for natural and isotopically pure h-BN samples reported in Ref. [14] (3.8 and 1.3 cm^{-1}, respectively) agrees very well with the underestimation of the isotopical disorder broadening by perturbation theory. Therefore, we conclude that the background impurity contribution to the FWHM is essentially the same for all isotopic compositions, contrary to previous analysis suggesting that the natural composition sample could have incorporated a higher impurity concentration on account of differences in the growth process [14].

Our results highlight the importance of isotopic disorder scattering in limiting the optical-phonon lifetime in h-BN. The E_{2g}^{high} phonon lifetime τ can be extracted from the FWHM of the Raman line using the uncertainty relation $\tau = \hbar/\Gamma_{\text{R}}$, where $\hbar = 5.30885 \times 10^{-12}$ cm^{-1} s is the Plank's constant and Γ_{R} is the FWHM of the Raman peak. The anharmonic and background impurity scattering contributions to the Raman line width ($\hbar/\tau_{\text{anh}}$ and $\hbar/\tau_{\text{imp}}$, respectively) are separated by analyzing the temperature dependence of the FWHM in isotopically pure samples. Assuming the same background impurity contribution irrespective of the isotopic composition, the isotopic-disorder-induced finite phonon lifetime τ_{iso} is derived from the FWHM of the isotopically mixed samples. In Fig. 4, the different contributions to the limited phonon lifetime are plotted for all the isotopic compositions studied. Whereas anharmonic decay and impurity background stand on the same footing, each limiting the phonon lifetime to about 4–5 ps, the isotopic disorder severely limits the phonon lifetime. Only in the sample with $x = 0.1$ the isotopic-disorder contribution is similar to that of anharmonic decay and impurity background. For the rest of isotopically mixed crystals, the isotopic disorder effect is dominant and the actual measured phonon lifetime follows closely the isotopic-disorder-limited lifetime τ_{iso}. It is then clear that further efforts to increase optical-phonon lifetimes by improving the crystalline quality, which are essential to enhance the performance of polaritonic devices, should be directed to isotopically pure crystals. Our study suggests ^{10}BN as the principal target, since it exhibits a slightly higher E_{2g}^{high} phonon lifetime and is less affected by a residual presence of the other boron isotope.

In summary, we have shown that isotopic disorder effects are prominent in h-BN by measuring the E_{2g}^{high} phonon linewidth for a set of isotopically mixed samples covering the whole range of isotopic compositions. The broadening of the phonon line width exhibits an asymmetric dependence on the isotopic composition with a maximum at $x \sim 0.65$ that cannot be explained by conventional perturbation theory up to third order. Good agreement with the observed Raman line widths and frequencies is achieved by considering a multiple-scattering theory based on the CPA. This underlines the strength of the isotopic-disorder-induced scattering and the prevalence of multiple-scattering in the h-BN crystal and should encourage further studies of wave interference effects on the thermal conduction of isotopically controled h-BN. Isotopic disorder scattering plays a crucial role in limiting the optical-phonon lifetime in isotopically mixed crystals, and is particularly relevant in mixed crystals with very low fraction of ^{10}B atoms. Then, the isotopically pure ^{10}BN crystal is the best candidate to achieve an en-

hancement of optical-phonon lifetimes, which is critical for phonon-polariton applications, by foreseeable advances in the h-BN crystal quality in the future. This work gives insight into the significance of isotopic-disorder scattering in limiting phonon lifetimes in the h-BN, and opens the prospect of similar studies in other layered compounds in which isotopic substitution is currently under intense investigation.

ACKNOWLEDGMENTS

This work has been supported by the Spanish MINECO/FEDER under Contract No. MAT2015-71035-R. Support for the h-BN crystal growth from the Materials Engineering and Processing program of the National Science Foundation, award number CMMI 1538127 is greatly appreciated.

---

[1] S. Chen, Q. Wu, C. Mishra, J. Kang, H. Zhang, K. Cho, W. Cai, A. A. Balandin, and R. S. Ruoff, Nat. Mater. **11**, 203 (2012).

[2] T. Q. P. Vuong, S. Liu, A. van de Lee, R. Cuscó, L. Artús, T. Michel, P. Valvin, J. H. Edgar, G. Cassabois, and B. Gil, Nat. Mater. **17**, 152 (2018).

[3] X. Li, J. Zhang, A. A. Puretzky, A. Yoshimura, X. Sang, Q. Cui, Y. Li, L. Liang, A. W. Ghosh, H. Zhao, et al., ACS Nano **13**, 2481 (2019).

[4] W. Wu, M. D. Morales-Acosta, Y. Wang, and M. T. Pettes, Nano Lett. **19**, 1527 (2019).

[5] M. Yankowitz, Q. Ma, P. Jarillo-Herrero, and B. J. LeRoy, Nat. Rev. Phys. **1**, 112 (2019).

[6] M. Cardona and M. L. W. Thewalt, Rev. Mod. Phys. **77**, 1173 (2005).

[7] J. D. Caldwell, I. Aharonovich, G. Cassabois, J. H. Edgar, B. Gil, and D. N. Basov, Nat. Rev. Mater. **4**, 552 (2019).

[8] A. Segura, L. Artús, R. Cuscó, T. Taniguchi, G. Cassabois, and B. Gil, Phys. Rev. Mater. **2**, 024001 (2018).

[9] J. D. Caldwell, A. V. Kretinin, Y. Chen, V. Giannini, M. M. Fogler, Y. Francescato, C. T. Ellis, J. G. Tischler, C. R. Woods, A. J. Giles, et al., Nat. Commun. **5**, 5221 (2014).

[10] A. Segura, R. Cuscó, T. Taniguchi, K. Watanabe, G. Cassabois, B. Gil, and L. Artús, J. Phys. Chem. C **123**, 17491 (2019).

[11] P. Li, M. Lewin, A. V. Kretinin, J. D. Caldwell, K. S. Novoselov, T. Taniguchi, K. Watanabe, F. Gaussmann, and T. Taubner, Nat. Commun. **6**, 7507 (2015).

[12] A. J. Giles, S. Dai, I. Vurgaftman, T. Hoffman, S. Liu, L. Lindsay, C. T. Ellis, N. Assefa, I. Chatzakis, T. L. Reinecke, et al., Nat. Mater. **17**, 134 (2018).

[13] R. Cuscó, J. H. Edgar, S. Liu, G. Cassabois, B. Gil, and L. Artús, Phys. Rev. B **99**, 085428 (2019).

[14] R. Cuscó, L. Artús, J. E. Edgar, S. Liu, G. Cassabois, and B. Gil, Phys. Rev. B **97**, 155435 (2018).

[15] F. Widulle, J. Serrano, and M. Cardona, Phys. Rev. B **65**, 075206 (2002).

[16] K. C. Hass, M. A. Tamor, T. R. Anthony, and W. F. Banholzer, Phys. Rev. B **45**, 7171 (1992).

[17] J. Spitzer, P. Etchegoin, M. Cardona, T. Anthony, and W. Banholzer, Solid State Comm. **88**, 509 (1993).

[18] S. Rohmfeld, M. Hundhausen, L. Ley, N. Schulze, and G. Pensl, Phys. Rev. Lett. **86**, 826 (2001).

[19] D. W. Taylor, Phys. Rev. **156**, 1017 (1967).

[20] R. He, L. Xue, J. Li, B. Liu, and J. H. Edgar, Chem. Mater. **30**, 6222 (2018).

[21] ABINIT is a common project of the Université Catholique de Louvain, Corning Incorporated, and other contributors (http://www.abinit.org). X. Gonze, J.-M. Beuken, R. Caracas, F. Detraux, M. Fuchs, G.-M. Rignanese, L. Sindic, M. Verstraete, G. Zerah, F. Jollet, et al., Comput. Mater. Sci. **25**, 478 (2002).

[22] R. Cuscó, B. Gil, G. Cassabois, and L. Artús, Phys. Rev. B **94**, 155435 (2016).

[23] A. A. Maradudin and S. Califano, Phys. Rev. B **48**, 12628 (1993).

[24] P. N. Sen and W. M. Hartmann, Phys. Rev. B **9**, 367 (1974).

[25] M. T. Pettes, M. M. Sadeghi, H. Ji, I. Jo, W. Wu, R. S. Ruoff, and L. Shi, Phys. Rev. B **91**, 035429 (2015).

[26] I. Savić, N. Mingo, and D. A. Stewart, Phys. Rev. Lett. **101**, 165502 (2008).